Proceedings of the ASME 2018 International Design Engineering
Technical Conferences and Computers and Information in Engineering Conference
IDETC/CIE 2018
August 26-29, 2018, Quebec City, Quebec, Canada

DETC2018-86374

DESIGN OF A NOVEL TORSIONAL SPRING FOR THE NEXT GENERATION COMPLIANT ACTUATORS

Jeong H. Yoon
Robotics and Mechanisms Laboratory
Department of Mechanical and Aerospace Engineering
University of California
Los Angeles, California 90095
Email: castring2018@gmail.com

Dennis Hong, Ph.D.
Robotics and Mechanisms Laboratory
Department of Mechanical and Aerospace Engineering
University of California
Los Angeles, California 90095
Email: dennishong@ucla.edu

ABSTRACT

Series Elastic Actuators (SEA) are one of the most widely studied compliant actuators in anthropomorphic robots and prostheses. However, due to the nature of its unique configuration, an unavoidable trade-off has to be made between compliance and bandwidth performance. In this paper, we show that by adopting a hypocycloid mechanism in rotary actuator designs, compliance and high force control bandwidth can be achieved at the same time, while reaping all the benefits of energy storage and shock absorption characteristics of mechanical springs.

NOMENCLATURE

T torque
F force
E energy
K stiffness
M motor
G gear
SC spring chassis
J inertia
Θ_d deflection angle
Θ_i initial angle
r planet gear radius
n number of planet gear pairs
d spring displacement
p preload displacement
$*_m$ quantities associated with the motor
$*_s$ quantities associated with the spring
$*_e$ quantities associated with extension
$*_c$ quantities associated with compression
$*_p$ proximal, the end of the actuator closer to robot base
$*_d$ distal, the end of the actuator closer to end effector

1. INTRODUCTION

Compliant actuators are widely investigated in current robotic platform developments thanks to its operational capability in a highly unstructured environment. There is increasing interest among researchers to design humanoid robots with compliant actuators which are able to perform a task in an unknown environment. These compliant actuators are often required to have a high torque output due to a heavy weight of the robots. This is one of the reasons why electromechanical Series Elas-

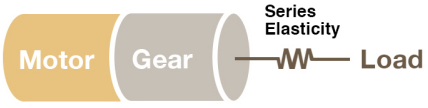

FIGURE 1. SCHEMATIC OF SERIES ELASTIC ACTUATOR [1]

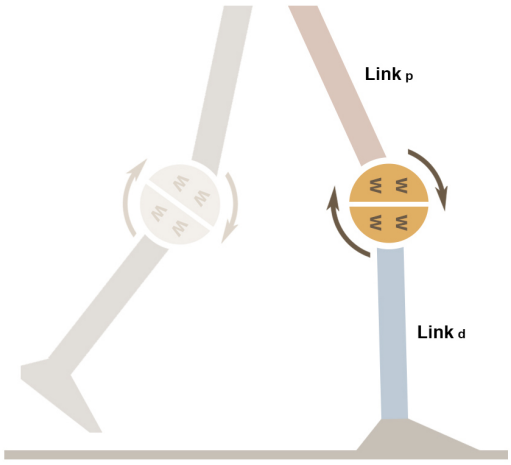

FIGURE 2. BIPEDAL WALKING ROBOT IN SINGLE SUPPORT PHASE [1]

tic Actuator (SEA) has been largely studied by many researchers worldwide ever since its emergence in 1995 [2]. In a SEA (Fig. 1), a high torque output is achieved with the high reduction gear box, and a mechanical compliance (spring) placed in series acts as a low pass filter to environment disturbances which is an essential feature when operating in unknown environments. However, due to the limitations imposed by this unique hardware configuration, most SEAs do not fully utilize the advantages of compliant actuators. To be specific, there are three main advantages of compliant actuators: increased force control fidelity, increased shock absorption and energy storage. Apparently, these advantages can be maximized when the actuator is more compliant. However, most SEAs in humanoids are required to use a very stiff spring because a large force/torque has to be transmitted through a spring in a series connection. This means that when a humanoid robot is in a single support phase as shown in Fig. 2, a single mechanical spring has to be stiff enough to hold up the entire weight of the body without spring saturation while the torque is transmitted. Further, compliant springs act as a low pass filter not only to the environment disturbances but also to the force/torque output from the gearbox, which inevitably lowers the force control bandwidth. Due to this limitation, some of the most advanced humanoid platforms developed recently use a very stiff spring such as a titanium beam [3] or titanium bar [4]. While such a stiff spring increases force control bandwidth, unnecessarily high stiffness yields a small deflection. Small deflections of the spring does not store large enough energy nor absorb shocks from the environment. This contradicting relationship between compliance and bandwidth has been considered an inevitable engineering trade-off [2]. Thus recently, stiffness selection criteria has become a new focus of SEA research in order to maximize the benefits of compliance while minimizing the cost in bandwidth reduction [1, 5, 6]. On the other hand, this paper suggests a completely different and innovative approach that attempts to solve the said problem.

2. DESIGN OF A NOVEL TORSIONAL SPRING

2.1 Hypocycloid Torsional Spring

A proposed hypocycloid torsional spring is based on the conventional hypocycloid mechanism with some modifications. The design consists of the customized planet and ring gear and springs connected in between them. A simplified simulation model is shown in Fig. 3. The pitch diameter of each planet gear is exactly half of the pitch diameter of the ring gear. In this configuration, a point on the circumference of the planet gear follows a straight line when it rolls inside the ring gear. In this torsional spring design, the two layers of planet gears are rigidly connected and roll as one piece. An antagonistic configuration was achieved

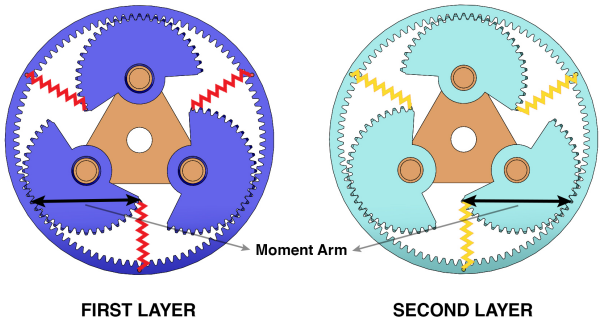

FIGURE 3. HYPOCYCLOID TORSIONAL SPRING SIMPLIFIED MODEL

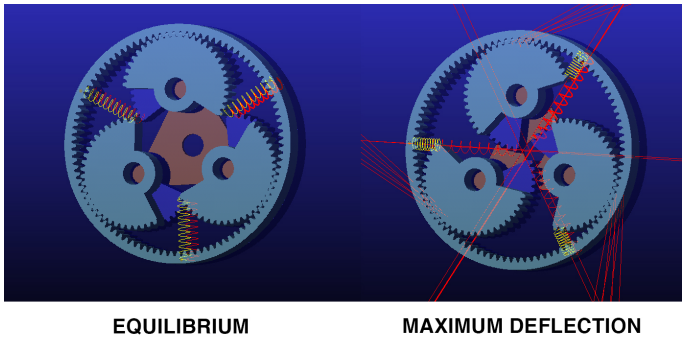

FIGURE 4. HYPOCYCLOID TORSIONAL SPRING SIMULATION

by attaching springs on two opposite sides of planet gears. As one spring moves away from the center, the other moves to the center just as flexors and extensors work in human muscles. The design was verified in ADAMS as shown in Fig. 4. The simulation shows the spring deflection from the equilibrium state to the maximum deflection state as 150 Nm torque was applied at the ring gear in a clockwise direction. As can be seen, as one side's spring compresses, the other side's spring extends. The generated spring forces and gear contact forces are shown as straight lines. It should noted that even though the gear ratio between the ring gear and each planet is 1:2, the gear ratio between the ring gear and the carrier is 1:1. Thus, the input torque to the ring gear remains same at the carrier output. In this simulation setting, the ring gear has a module of 1 and 96 teeth, the planet gear has a module of 1 and 48 teeth, and the spring stiffness is 42380.7 N/m with a preload of 269.1 N. The spring used in the simulation is based on the actual spring (model number: 306-205-D) from the Associated Spring Raymond, which has a free length of 32 mm (1.26 in) and a saturated length of 19.3 mm (0.76 in). The equilibrium point is set at the middle where the length is 25.4 mm (1.0 in). The antagonistic configuration with the preload is used in the design so that when the spring is extended from the equilibrium point for a targeted degree deflection, there still remains some preload on the spring. This is because the spring force is not reproducible for very small deflections, and nonlinear behavior begins as the number of active turns diminishes as coils begin to touch [7]. A more descriptive prototype model is shown in Figs. 5 and 6. In order to avoid interference among planet gears, the planet gears were customized in shape as shown in Fig. 6 in the prototype design. These highly customized planet and ring gears are planned to be machined using wire EDM.

A more conventional hypocycloid mechanism was once used in other actuator design [8], however, they only focused on utilizing the nonlinear torque profile of a single extension spring for jumping motions, which is inherent in the hypocycloid mechanism that combines rotary and linear motions. In our work, the hypocycloid mechanism was used with compression springs that are placed in an antagonistic configuration to make a pancake-shaped spring, which also generates a linear torque profile and can be attached to actuators as an independent unit.

This novel hypocycloid torsional spring has numerous advantages over conventional torsional springs. First, a more stiff and compact form is possible since compression springs exhibit higher volumetric and mass energy densities [9]. Secondly, compression springs do not buckle when being compressed inside the hypocycloid mechanism since they expand and compress along a straight line. The buckling of the compression spring has been a significant factor that inhibited large deflection in rotary form actuator designs [10]. Moreover, the effective stiffness is amplified in the hypocycloid mechanism since a moment arm is generated from the spring to the point where the planet gear engages with the ring gear as shown in Fig. 3. This implies that a very stiff

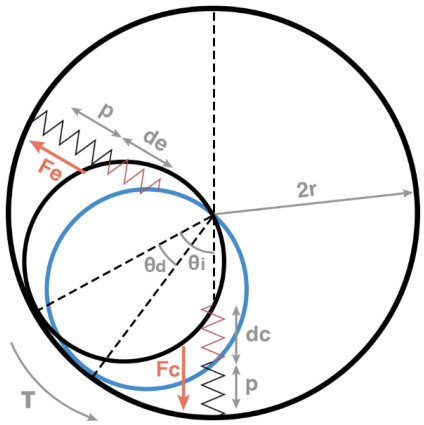

FIGURE 5. SCHEMATIC OF HYPOCYCLOID SPRING MECHANISM

torsional spring of a compact size can be designed with off-the-shelf compression springs. Third, high bandwidth performance can be achieved since torque is transmitted through rigid bodies while spring forces pass through the center of the actuator and does not interfere with the transmitted torque. This topic will be revisited and further explained in the section 4.1.

The author's previous work [1] focused on establishing a spring selection criteria based on the newly identified unlumped model for rotary form SEAs. In short, the design criteria implies that one can use approximately 10 times more compliant springs than titanium beams without sacrificing the quality of force control if the spring chassis inertia is kept small. However, it has to be noted that the stiffness of such a spring is still fairly high and no torsional spring of a compact size that are available in the market can meet this criteria. This is reasonable considering the fact the a required torque of a knee actuator for a 80kg humanoid robot to clime up stairs is around 150 Nm [11], while a required torque for a 75kg human to jump is around 200 Nm [12]. As mentioned in [13], this is a considerably large amount of torque since the torque from a 1270 kg Toyota Corolla is 170 Nm at 4000 rev/min. The hypocycloid torsional spring is the most compact form torsional spring up to date that can meet this criteria.

2.2 Torque Deflection Curve

The below equations show the relationship between elastic deflection and elastic torque based on the schematic diagram shown in Fig. 5. It has to be noted that the spring extension length is not same as the spring compression length when three planet gears are used. It is because the initial angle is not equal to zero when the planet gear is placed at an angle. The extension is always slightly larger than the compression length in this con-

figuration, so the targeting deflection angle is determined by the maximum extension length possible. Nevertheless, three planet gears were used in the prototype design in order to successfully distribute the load based on the gear teeth strength.

The below equations (1)-(3) are for compression.

$$d_c = 2r\cos(\Theta_i - \Theta_d) - 2r\cos(\Theta_i) \quad (1)$$

$$F_c = K(d_c + p) \quad (2)$$

$$T_c = F_c 2r\sin(\Theta_i - \Theta_d) \quad (3)$$

The below equations (4)-(6) are for extension.

$$d_e = 2r\cos(\Theta_i) - 2r\cos(\Theta_i + \Theta_d)) \quad (4)$$

$$F_e = K(p - d_e) \quad (5)$$

$$T_e = F_e 2r\sin(\Theta_i + \Theta_d) \quad (6)$$

The total torque generated from the elastic deflection can be calculated as the below equation (7), where n stands for the number of planet gear pairs.

$$T_{total} = n(T_c + T_e) \quad (7)$$

2.3 Prototype Deign based on Targeted Torque and Deflection Angle

It has to be noted that when the pitch diameter of the ring gear is large, a large compression and extension length of the spring is required as well. Even though the simulation model shown in Fig. 4 is perfectly valid to study the mechanism behavior, the spring used in the simulation does not have enough stroke length to yield the targeted torque of 150 Nm before spring saturation. In order to decrease the stroke length for the targeted deflection, the ring gear and planet gears have to be reduced in size. In the prototype model shown in Fig. 6, the number of teeth of the ring gear and the planet gear was reduced approximately in half (46 for the ring gear, 23 for the planet gear) while the module of the gear remained same. This design change successfully took into account the stroke length of actual springs.

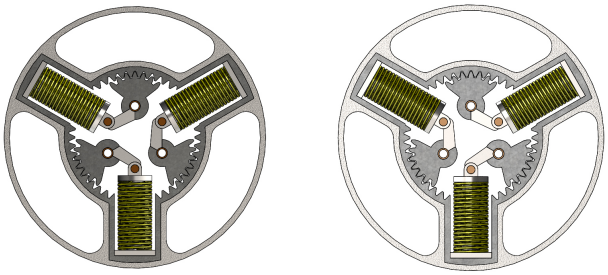

FIGURE 6. TWO LAYER SPRING CONFIGURATIONS

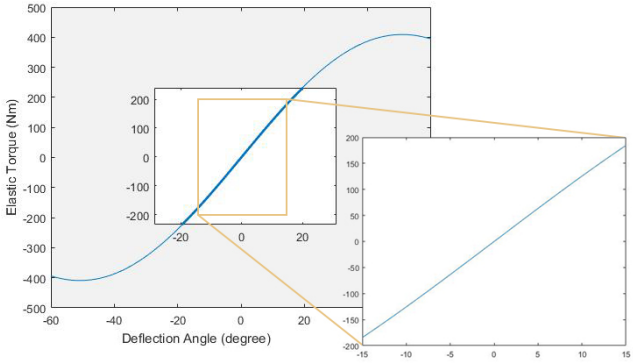

FIGURE 7. TORQUE DEFLECTION CURVE

However, when the ring gear size decreases, the moment arm length also decreases, which necessitates the use of more stiff spring. On the other hand, when a higher stiffness spring is used, the actuator size inevitably increases since springs have a bigger size. Then one may want to opt to use a single layer spring with fewer number of springs instead for compactness, which also inevitably decreases the torque amount. These are exemplary design parameters that need to be chosen carefully based on specific applications. There are a few other design parameters that need to be fine-tuned this way. For example, increasing the initial angle, Θ_i, increases the amount of measurable torque since it increases the moment arm length. However, the initial angle is also associated with stroke length and spring size. Moreover, spring stiffness, the number of planet gear pairs and the preload amount are all design parameters that affect one another. Since there are many design parameters that affect the performance outcome in a similar fashion, it is important to establish target specifications and their priorities for specific applications.

For a prototype model, a knee actuator of a 70 kg humanoid

robot was considered. Thus the output torque of 150 Nm was set as the primary goal. Achieving the largest deflection angle (±15) was chosen as the second priority. Based on these primary goals, one can choose a stiffer spring (model number 306-505-D from Associated Spring Raymond) for the configuration shown on Fig. 6. It can be verified from the equations (1)-(7) that the aforementioned specification meets the targeted values as shown in Fig. 7. These design parameters can be further optimized to include other design goals such as compactness.

The hypocycloid torsional spring can be treated as an independent unit and can be attached to a motor gear unit as shown in Fig. 8. The three core components of the compliant actuators are shown in this prototype model. The motor is the T-motor U8 KV100 which exhibits the maximum continuous stall torque of around 1.4 Nm. For gearbox, a double row planetary gear [14] was chosen as an alternative to the Harmonic or Cycloid Drive for a compact, low cost, and energy efficient actuator. The gear ratio was designed to be 1:126, which makes the maximum continuous output torque of 176 Nm. The output of the double row planetary gearbox is the second layer ring gear, and it is rigidly connected to the spring chassis which contains a T-shaped hypocycloid torsional spring. The gear box output and the spring chassis are shown as transparent parts. The output torque from the gearbox will be transmitted through the hypocycloid spring to the carrier output which is shown as another highlighted transparent part.

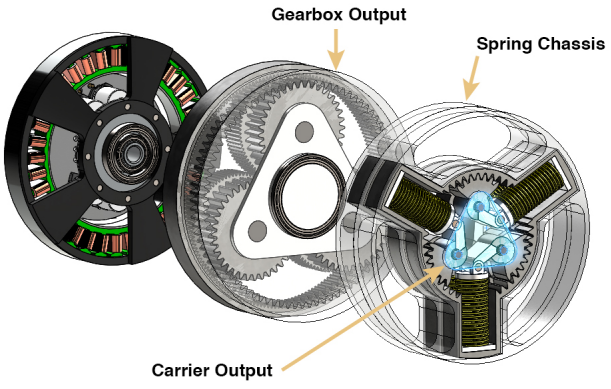

FIGURE 8. PROTOTYPE ACTUATOR MODEL

3. EXPECTED PERFORMANCE IMPROVEMENTS

3.1 Force Control

It has to be noted that the configuration of the new compliant actuator is different from the conventional SEAs. The new actuator design still has the two degrees of freedom just like an SEA:

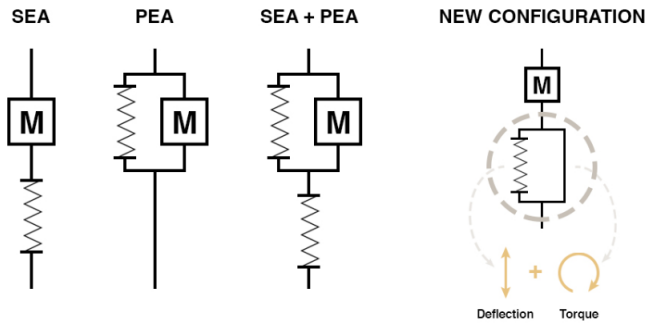

FIGURE 9. ELASTIC ACTUATOR CONFIGURATION COMPARISON

one is at the motor output and the other at the spring deflection. However, the spring is no longer in a series connection, but rather in a parallel configuration with the ring and planet gear pairs in the spring chassis. The new configuration is shown in Fig. 9 along with SEA and PEA (Parallel Elastic Actuator) [15] for comparison. In this configuration, the torque transmittance is decoupled from the spring deflection, and the torque is transmitted immediately through the ring and planet gears to the load since the two rigid bodies are consistently in contact with each other. Further, since spring forces pass through the center of the actuator, they do not interfere when the torque is transmitted from the ring gear to the carrier. The transmitted torque at the carrier forces the planet gear to rotate and compresses/extends the springs, which gives a means to measure the transmitted torque. The planet gear rolls until the elastic torque generated from the spring deflection balances the transmitted torque. This was confirmed through a series of ADAMS simulations, and one of them is shown in Fig. 10. In this model simulation, the input torque of 150 Nm was applied at the ring gear as a step function, and the transmitted torque at the carrier was read. It shows that the input and output torque have the same magnitude but are in the opposite direction. When superimposed, the input and output torque

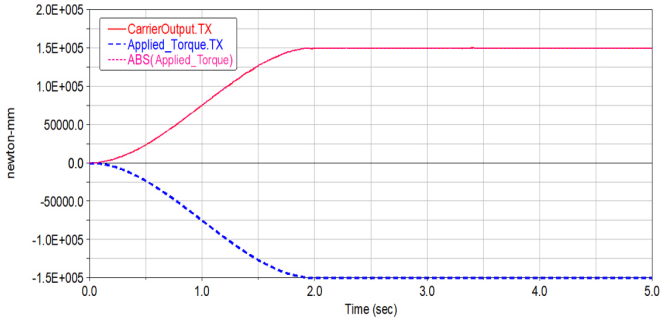

FIGURE 10. TRANSMITTED TORQUE AT CARRIER OUTPUT

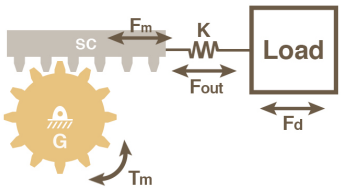

a) Conventional SEA

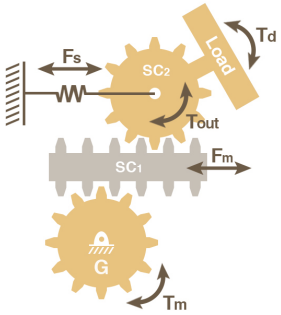

b) New Compiant Actuator

FIGURE 11. LINEAR REPRESENTATION OF ROTARY ACTUATORS

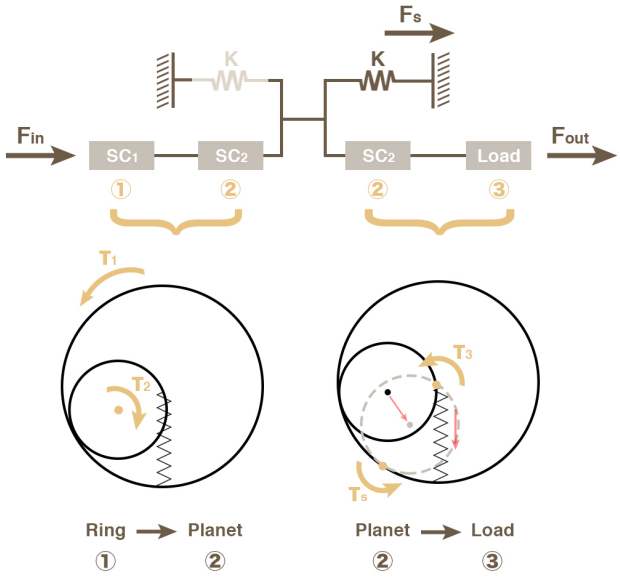

FIGURE 12. FORCE/TORQUE FLOW DIAGRAM

exactly match since torque transmittance is immediate. When the transmitted torque reached 150 Nm at 2 seconds, the planet gears stopped rolling.

To help facilitate visualization, more intuitive linear representation of the actuator model based on the rack and pinion model [16] is shown in Fig. 11. In this new configuration, the ring and planet gears can be thought of as an extension of the spring chassis (SC1 is the ring gear, SC2 is the planet gear) and also as a *moving* spring chassis that is directly connected to the load and the spring. In this linearized model, motor torque is transmitted through the spring chassis 1 which is represented as a rack. This can be considered as a ring gear that has infinite radius. The spring chassis 2 rolls without slipping on the spring chassis 1. As it rolls, rotational motion transmits the output torque to the load while translational motion deflects the spring. Note that the translational motion is visualized here to better illustrate the mechanism. However, it should be noted that the planet gear only rolls inside the ring gear and the spring is deflected along a straight line with the hypocycloid mechanism.

The force/torque flow diagram of the mechanism is further illustrated in Fig. 12. When the torque is transmitted from the ring gear to the planet gear and to the load, the transmittance is immediate since the stiffness of the planet gear is much higher than that of the spring. Also, one end of the spring can be considered fixed to the ground as no force/torque is transmitted from that end. In this configuration, the spring no longer acts as a low pass filter to the input torque since the force/torque is directly transmitted through rigid bodies. It only acts as a sensor that measures the transmitted force/torque.

Since the stiffness of the gear pair is much higher than that of the springs, the bandwidth frequency of the system will largely depend on the stiffness of the gear pairs in the spring chassis and will be much higher than the one from conventional SEAs. The verification of the force control bandwidth from the proximal link to the distal link as in [16] remains as a future work since a completely rigid body was assumed for gears in our simulation.

3.2 Energy Storage

The amount of energy stored in a spring is proportional to the square of the deflection distance. Since a large deflection can be achieved with compression springs in the hypocycloid torsional spring, large amounts of energy can be stored in the system. Based on Castigliano's Theorem [7], we get the following equation for the potential energy.

$$E = \int_0^{\Theta_d} T_{total} d\Theta_d \tag{8}$$

Based on the aforementioned specification, the actuator is expected to store around 40 J at the maximum deflection.

The highly regarded compliant joint design (VS joint) [17] has a similar performance outcome to the hypocycloid torsional

spring in terms of the maximum output torque and angular displacement. However, the hypocycloid torsional spring is much more compact and light weight, while it is capable of storing twice as much energy than the VS joint.

The large amount of energy stored in a much more compact and lightweight actuator will eventually help better assist walking in humanoids.

3.3 Shock Absorption

The shock absorption capability of the hypocycloid spring was observed through a simple free fall of a pendulum simulation as shown in Fig. 13. The long pendulum extended from the actuator mimics a limb attached to the actuator. In simulation, the pendulum fell due to gravity while the actuator was held fixed. The contact force at the moment of impact from the free fall was observed as shown in Fig. 14. As can be seen, the impact force is evenly distributed to the planet gear pair in the spring chassis and the spring.

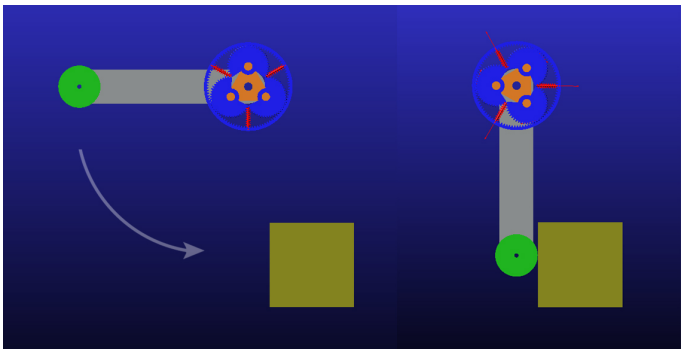

FIGURE 13. IMPACT SIMULATION

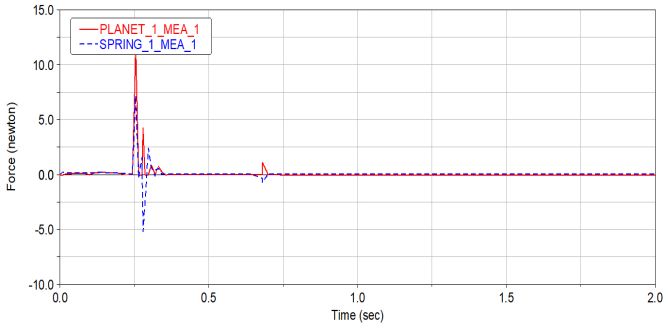

FIGURE 14. IMPACT FORCE GRAPH

The effect of a low reduction gear in impact mitigation was thoroughly studied in the MIT Cheetah actuator [13]. While the MIT Cheetah actuator absorbs impact through a back-driving motor and a low reduction gear, the hypocycloid torsional spring absorbs impact through the low reduction gear pair in the spring chassis and springs

4. CONCLUSION

By combining the hypocycloid mechanism with compression springs, a novel torsional spring was designed. The proposed design showed that a high stiffness and compact lightweight torsional spring can be designed to satisfy a high torque output with a large angular displacement. The maximized angular displacement can be used to store a large amount of energy upon deflection and successfully absorb shocks. Further, this design is expected to overcome the engineering trade-off between compliance and bandwidth performance that was once considered unavoidable in SEA designs.

5. FUTURE WORK

The prototype design is expected to be improved through optimization and iteration process. The actuator will also be manufactured in house using CNC machine and wire EDM. Its performance will be experimentally verified and compared to conventional SEAs.

ACKNOWLEDGMENT

We would like to acknowledge our gratitude to the MSC corporation for providing an Adams license, and the Office of Naval Research, through whom this research was funded and made possible. This work was partially supported by ONR Award Number N00014-15-1-2064.

REFERENCES

[1] Yoon, J. H., Sun, D., Sanandan, V., and Hong, D., 2017. "Experimental validation of unlumped model and its design implications for rotary series elastic actuators". *Volume 5A: 41st Mechanisms and Robotics Conference*, Jun.

[2] Pratt, G. A., Williamson, M. M., Dillworth, P., Pratt, J., and Wright, A., 1997. "Stiffness isnt everything". *Experimental Robotics IV Lecture Notes in Control and Information Sciences*, p. 253262.

[3] Lee, B., Knabe, C., Orekhov, V., and Hong, D., 2014. "Design of a Human-Like Range of Motion Hip Joint for Humanoid Robots". *Volume 5B: 38th Mechanisms and Robotics Conference*.

[4] Negrello, F., Garabini, M., Catalano, M. G., Malzahn, J., Caldwell, D. G., Bicchi, A., and Tsagarakis, N. G.,

2015. "A modular compliant actuator for emerging high performance and fall-resilient humanoids". *2015 IEEE-RAS 15th International Conference on Humanoid Robots (Humanoids)*.

[5] Orekhov, V. L., Knabe, C. S., Hopkins, M. A., and Hong, D. W., 2015. "An unlumped model for linear series elastic actuators with ball screw drives". *2015 IEEE/RSJ International Conference on Intelligent Robots and Systems (IROS)*.

[6] Roozing, W., Malzahn, J., Kashiri, N., Caldwell, D. G., and Tsagarakis, N. G., 2017. "On the stiffness selection for torque-controlled series-elastic actuators". *IEEE Robotics and Automation Letters,* ***2***(4), p. 22552262.

[7] Budynas, R. G., Nisbett, J. K., and Shigley, J. E., 2011. *Shigleys mechanical engineering design*. McGraw-Hill.

[8] Thorson, I., and Caldwell, D., 2011. "A nonlinear series elastic actuator for highly dynamic motions". *2011 IEEE/RSJ International Conference on Intelligent Robots and Systems*.

[9] Rouse, E. J., Mooney, L. M., Martinez-Villalpando, E. C., and Herr, H. M., 2013. "Clutchable series-elastic actuator: Design of a robotic knee prosthesis for minimum energy consumption". *2013 IEEE 13th International Conference on Rehabilitation Robotics (ICORR)*.

[10] Tsagarakis, N., Laffranchi, M., Vanderborght, B., and Caldwell, D., 2009. "A compact soft actuator unit for small scale human friendly robots". *2009 IEEE International Conference on Robotics and Automation*.

[11] Knabe, C., Griffin, R., Burton, J., Cantor-Cooke, G., Dantanarayana, L., Day, G., Ebeling-Koning, O., Hahn, E., Hopkins, M., Neal, J., and et al., 2017. "Team valors escher: A novel electromechanical biped for the darpa robotics challenge". *Journal of Field Robotics,* ***34***(5), p. 912939.

[12] Tsiokanos, A., Kellis, E., Jamurtas, A., and Kellis, S., 2002. "The relationship between jumping performance and isokinetic strength of hip and knee extensors and ankle plantar flexors". *Isokinetics Exercise Sci.,* ***10, no 2***, 11, pp. 107–115.

[13] Wensing, P. M., Wang, A., Seok, S., Otten, D., Lang, J., and Kim, S., 2017. "Proprioceptive actuator design in the mit cheetah: Impact mitigation and high-bandwidth physical interaction for dynamic legged robots". *IEEE Transactions on Robotics,* ***33***(3), p. 509522.

[14] Brassitos, E., and Mavroidis, C., 2013. "Kinematics analysis and design considerations of the gear bearing drive". *Advances in Mechanisms, Robotics and Design Education and Research Mechanisms and Machine Science*, p. 159175.

[15] Grimmer, M., Eslamy, M., Gliech, S., and Seyfarth, A., 2012. "A comparison of parallel- and series elastic elements in an actuator for mimicking human ankle joint in walking and running". *2012 IEEE International Conference on Robotics and Automation*.

[16] Orekhov, V. L., Knabe, C. S., Hopkins, M. A., and Hong, D. W., 2015. "An unlumped model for linear series elastic actuators with ball screw drives". *2015 IEEE/RSJ International Conference on Intelligent Robots and Systems (IROS)*.

[17] Wolf, S., and Hirzinger, G., 2008. "A new variable stiffness design: Matching requirements of the next robot generation". *2008 IEEE International Conference on Robotics and Automation*.